Cancer Immunology, Immunotherapy
https://doi.org/10.1007/s00262-020-02640-6

ORIGINAL ARTICLE

A single-valent long-acting human CD47 antagonist enhances antibody directed phagocytic activities

Fenglan Wu[1] · **Yangsheng Qiu**[1] · **Yuhong Xu**[1,2]

Received: 21 May 2019 / Accepted: 13 June 2020

Abstract

Many cancer cells express CD47 as a 'don't eat me' signal to mask their presences from immune recognition and destruction. Such a signal is transmitted when CD47 binds to the signal regulatory protein-α (SIRPα) on macrophages to cut the phagocytic reaction. Most recent studies have focused on developing CD47 blocking agents with different affinities and avidities in order to optimize the therapeutic window between efficacy and toxicities involving normal cells expressing CD47. We described in this study a new design to fuse one CD47 binding domain of SIRPα with a pharmacokinetics modifying domain F8. The resulted single valent long-acting CD47 antagonist SIRPα-F8 was able to bind to CD47 and disrupt CD47-SIRPα axis. However, by itself it cannot trigger endocytosis and has no effect on tumor growth. Only when used in combination with the anti-CD20 mAbs, there were greatly improved phagocytic activities towards CD20 positive cancer cells. In vivo the combination also resulted in better tumor growth inhibition comparing to the vehicle control group. In addition, we showed that the F8 fusion bound to hFcRn only inside endosomes at pH 6.0, enabled hFcRn mediated recycling and thus greatly extended the circulation half-life in hFcRn knock-in mice. Taken together, the SIRPα-F8 design may suggest a new option to improve the therapeutic index of antibody treatment in clinical use towards tumors.

Keyword Long-acting · CD47 antagonist · Therapeutic mab · FcRn · anti-CD20

Abbreviations

AUC	Area under the curve
FcRn	Neonatal Fc receptor
i.t.	Intra tumoral
M-CSF	Macrophage colony-stimulating factor
MDS	Myelodysplastic syndromes
MRT	Mean residence time
PK	Pharmacokinetic
RCC	Renal cell carcinoma
SEC	Size exclusion chromatography
SIRPα	Signal regulatory protein-α
TGI	Tumor growth inhibition

Electronic supplementary material The online version of this article (https://doi.org/10.1007/s00262-020-02640-6) contains supplementary material, which is available to authorized users.

✉ Yuhong Xu
yhxu@dali.edu.cn

[1] School of Pharmacy, Shanghai JiaoTong University, Shanghai, People's Republic of China

[2] School of Pharmacy and Chemistry, Dali University, Dali, YunNan, People's Republic of China

Introduction

Many therapeutic monoclonal antibody (mAb) drugs have been developed to target cancer cell surface antigens and exert anti-tumor effects via ADCC effector function. However, cancer cells may find ways to escape immune destruction by hijacking endogenous immune checkpoint pathways used by the host to maintain self-tolerance [1]. Checkpoint inhibitors including anti-CTLA4 and anti-PD-1 have shown remarkable clinical success [2–4]. But they were both targeted to T cell mediated adaptive immune responses. There should be other immune regulatory pathways implicated in cancer development especially concerning the innate immunity.

Macrophages are important players in both innate and adaptive immunities [5]. The phagocytic activities via the 'large eaters' are regarded as essential anti-tumor immune functions. Some cancer cells were found to block macrophage mediated phagocytosis by expressing CD47 as the so-called 'don't eat me' signal [6, 7]. CD47 is a ubiquitous cell surface marker found on many 'self' cells. It interacts with the signal-regulatory protein α (SIRPα) on macrophages, DCs and neutrophils as a major myeloid-specific

Published online: 24 June 2020

immune checkpoint [8, 9]. High CD47 expression on cancer cells was found to be a major barrier for immune recognition, and the antibody-dependent cellular phagocytosis (ADCP) effects in cancer therapy [10–13].

Based on these findings, several groups are developing CD47 blocking antibodies to disrupt the CD47-SIRPa checkpoint axis [14–16]. The most advanced mAb 5F9 had shown significant anti-tumor effects in a phase I/II trial but there were also reports of hematological toxicities [17]. These side effects were thought to be due to the high CD47 expression levels on red blood cells and related Fc effector functions against normal cells. Various other designs including SIRPα-Fc and different IgG variants were under evaluation for reduced toxicity and improve efficacy [18–20]. We described in this study the design of a single valent, long-acting, CD47 antagonist SIRPα-F8. The fusion protein contains an IgV domain of SIRPα as the 'eat me' module and an F8 scFv as the 'recycle me' module (Fig. 1d). The F8 is a human FcRn binding scFv only inside endosomes at pH 6.0. It was used to improve the circulation stability and half-life of a GLP1R agonist peptide [21]. The F8 fusion was found to have a mean residence time of up to

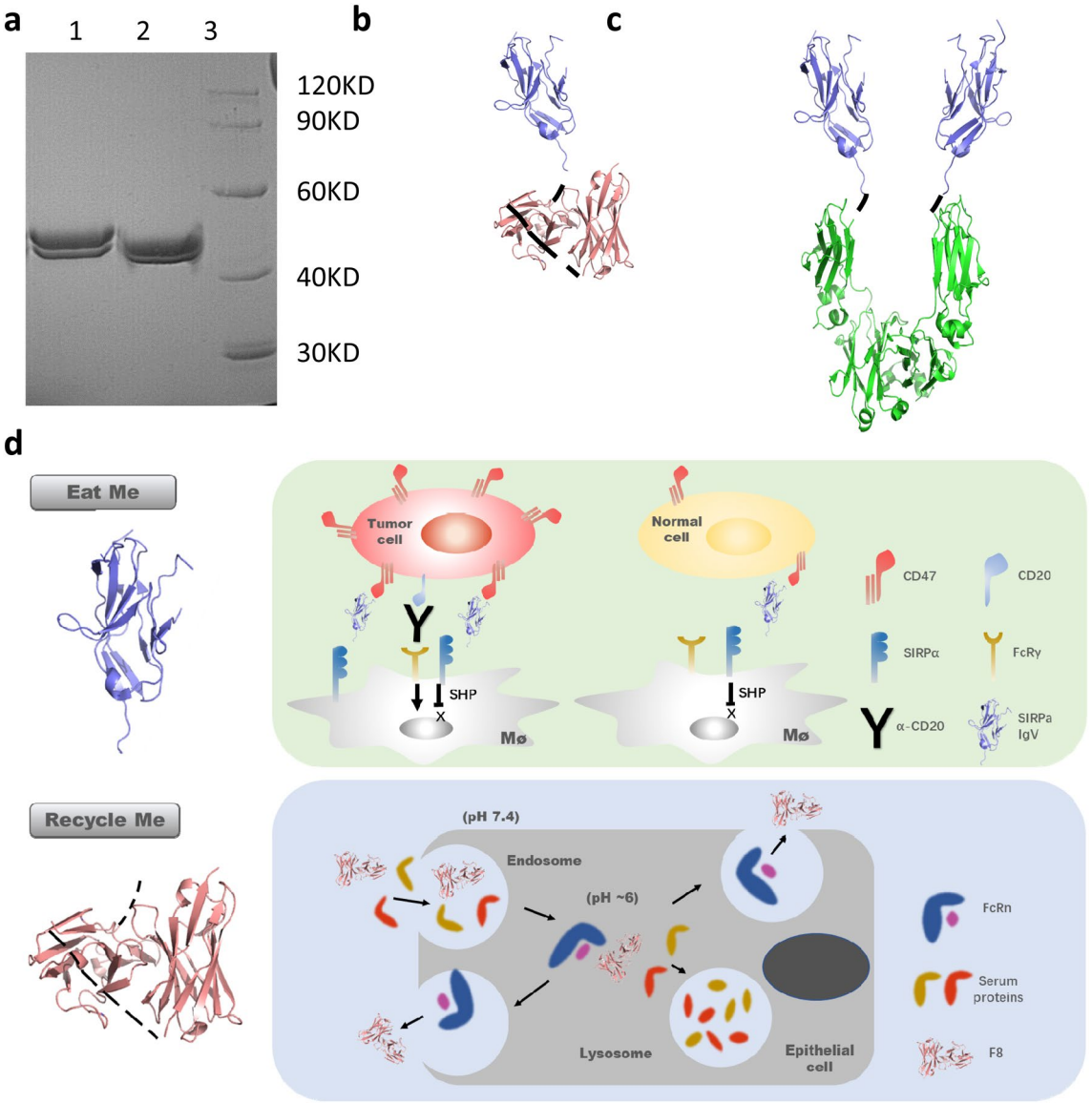

Fig. 1 SIRPα-F8 fusion protein design and proposed mechanism of action. **a** Gel electrophoresis characterization of the SIRPα-F8 fusion proteins. 1: SDS-PAGE; 2: Non-reducing PAGE; 3: Marker PAGE. **b** The design of SIRPα-F8. **c** The design of SIRPα-Ig. **d** Schematic illustration of the proposed SIRPα-F8 mechanism of action. The 'Eat me' module was designed to antagonize CD47 on cancer cell and block the inhibitory signal towards macrophage. The 'Recycle me' module was used to enable binding to FcRn at pH 6.0 in the endosome to escape lysosome degradation during circulation

238 h in primates. Therefore we designed the fusion protein SIRPα-F8 to explore a new way to adjust the therapeutic windows of CD47 blocker and improve the ADCP activities of tumor cell opsonizing antibodies.

Materials and methods

Proteins and antibodies

The IgV fragment of human SIRPα (P78324, Glu31-Ser149) was cloned with a C-terminal poly-histidine tag and expressed as SIRPα-His. The SIRPα-F8 fusion gene was designed to encode SIRPα IgV connected by a $(G_4S)_3$ linker with the F8 scFv sequence described previously [21]. Another two constructs containing a SIRPα with an irrelevant scFv (SIRPα-F0), or a SIRPα with the Fc fragment of human IgG4 (SIRPα-Ig) were also made. The cDNAs were all synthesized by Genscript, cloned into the pcDNA3.1 vector, and expressed using a HEK293-6E suspension cells expression system (ThermoFisher). The secreted proteins were harvested from the supernatants and purified using a HisTrap FF column on AKTA explorer (GE Healthcare). The quality of the fusion proteins was determined by BCA, SDS-PAGE and size exclusion chromatography (SEC). SIRPα-Ig was biotinylated following the instructions of the EZ-Link Sulfo-NHS-SS-Biotin kit (Thermo Scientific, 21,328). The anti-CD47 blocking antibody B6H12 and non-blocking antibody 2D3 were purchased from eBioscience. The anti-CD20 antibody was kindly provided by Huahai Pharmaceutical.

Cell lines

Stably transfected $293T^{EGFP-hFcRn}$ and $293T^{EGFP-HLA}$ cell lines were made in our laboratory as described previously [21]. Human CD47 expressing CHO cells ($CHO^{EGFP-hCD47}$) were obtained by transfecting the hCD47 cloning vector (Sino Biologicals) and culturing the transfected cells in medium containing hygromycin. NHL Raji cells and T lymphoblastoid leukemia CCRF-CEM cells were cultured using RPMI1640 medium with 10% fetal bovine serum (Gibco).

Cell binding assay and FACS analysis

SIRPα-F8 or SIRPα-F0 were added into $CHO^{EGFP-hCD47}$ or Raji cell cultures in 96-well plates at different concentrations. After incubation for 30 min at 4 °C, the cells were washed three times by cold PBS, and labeled with APC-conjugated mAbs against the His tag (1:2,000; Genscript) for 30 min at 4 °C. Finally, the cells were washed three more times with PBS, and examined for MFI using a BD Celesta FACS machine.

The competitive binding of SIRPα-F8 with SIRPα-Ig and the CD47 blocking antibody B6H12 were also done. The SIRPα-Ig was biotinylated and added into cell culture medium containing different concentration of SIRPα-F8. After incubation for 30 min, the cells were washed three times with cold PBS, labeled with APC conjugated streptavidin (1:5000, BioLegend) for 30 min at 4 °C, washed again for three times with PBS, and quantified based on MFI from FACS machine (BD FACSCelesta). Similarly, SIRPα-F8 binding in the presence of CD47 blocking antibodies were quantified and the blocking percentages were calculated. Data analysis was performed using PRISM Graphpad software.

$HEK293T^{EGFP-hFcRn}$ and $HEK293T^{EGFP-HLA}$ cells were incubated in a 96-well plate in the presence of increasing concentrations of SIRPα-Ig, SIRPα-F8 or SIRPα-F0 at pH6.0 or pH7.4. Meanwhile, 250 mg/ml CD47 protein were added into each well. Secondary APC conjugated anti-his mAb labeling and washing steps were all kept at pH6.0 or pH7.4. The resulted cell associated fluorescence intensity was analyzed using a BD Celesta FACS machine.

Phagocytosis assay and high-content cellomics imaging analysis

Human monocytes were purified from PBMC with CD14 microbeads (Miltenyi). Purified $CD14^+$ monocytes were cultured in the presence of macrophage colony-stimulating factor (M-CSF) for 7–10 days. Monocyte-derived macrophages were harvested by dissolving in dissociation buffer for 5 min with gentle scraping. They were then labeled with PKH26 (red) and plated in IMDM containing 10% FBS for 24 h followed by serum-free media for another 2 h. 5×10^4 CFSE-labeled Raji cells or CCRF-CEM cells were added into the well with the presence of various protein constructs. All proteins were used at the same concentration of 10 mg/ml. After 2 h of incubation, the cells were washed 3 times with IMDM and fixed with 2% PFA. The wells were scanned using the Cellomics high-content Imaging platform. The fluorescence images were analyzed using the HCS Studio Cell Analysis Software and the pre-established phagocytosis assay parameters. The phagocytosis index was determined by calculating the number of phagocytes per 100 macrophages as described in ref. 11. The data was plotted in Microsoft Office Excel and Graphpad Prism 5.

Animal models and animal studies

For setting up of the Raji xenograft model, 3×10^6 Raji cells were injected subcutaneously into the right flank of each 6- to 8-week-old NOD/SCID mouse. After the mice had

developed tumors with about 130 mm^3 volume, they were given three times per week injections of 200 ml vehicle (intra tumoral, i.t.), 200 mg SIRPα-F8 fusion protein (i.t.), 200 mg anti-CD20 (i.p.), or combination of 200 mg SIRPα-F8 fusion protein (i.t.) and 200 mg anti-CD20 (i.p.) for 3 weeks. Tumor volume was measured every 3–4 days using the formula (length*$width^2$)/2. Tumor growth inhibition (TGI) was calculated as TGI (%) = (Vc−Vt)/(Vc−Vo)*100, where Vc, Vt are the median of control and treated groups at the certain day of the study and Vo at the start.

Pharmacokinetics studies in hFcRn knock-in mice

Twelve hFcRn knock-in mice were purchased from Beijing Biocytogen Co., Ltd. and acclimated in the SPF animal room for 1 week. six mice were given a single intravenous bolus injection of 0.5 mg/kg endotoxin-free biotin labeled SIRPα-F8 in PBS. Another 6 mice received SIRPα-F0 at the same dose. Blood samples were taken at baseline (t_0), 10 min, 1, 4, 8, 24 h, 2, 4, 7, 14, 21 days after injection. Quantitative ELISA assays were conducted to determine the fusion protein concentration. Each sample was measured in three technical replicates. The data were plotted using ELISA concentration vs. time. $T_{1/2}$, AUC_{inf}, Clearance and Mean residence time (MRT) were analyzed based on the Linear Log Trapezoidal method, plasma (200–202) model (non-compartment model) using WinNonlin (Certara).

Results

Expression and characterization of the SIRPα-F8 fusion protein

The fusion protein containing the IgV fragment of human SIRPα connected to the F8 scFv and a 6XHis tag was made and designated as SIRPα-F8 (Fig. 1b). The proteins were expressed in HEK293-6E suspension cells expression system, purified and characterized. The SDS-PAGE of SIRPα-F8 was shown in Fig. 1a. The two bands in Fig. 1a suggested there might be two differently glycosylated proteins produced. The molecular weight of the SIRPα-F8 is 45 kD, which is about one third of that of an IgG.

The binding capability of SIRPα-F8 to CD47 was shown using both NHL Raji cells and $CHO^{EGFP-hCD47}$ cells (Fig. 2a, b). The Raji cells are known to be CD47 positive. The $CHO^{EGFP-hCD47}$ cells were obtained after stable transfection of the EGFP-hCD47 gene. The competition between SIRPα-F8 binding to Raji cells and those of SIRPα-Ig or CD47 antibody B6H12 were examined in Fig. 2c. In the left figure, SIRPα-Ig concentration was fixed at 100 nM and SIRPα-F8 were added at concentrations of 30, 10, 3.3 mg/ml. While SIRPα-F8 as a monomer had lower avidity, but it could still compete with SIRPα-Ig at higher doses. The right figure showed the effect of CD47 blocking antibody B6H12 on SIRPα-F8 binding. The SIRPα-F8 concentration was fixed at 560 nM, and the blocking percentages of B6H12 were reported.

We also examined the binding affinity of SIRPα-F8 to human FcRn. SIRPα fusion with an irrelevant scFv labeled as SIRPα-F0 was included as a negative control. $293T^{EGFP-hFcRn}$ and $293T^{EGFP-HLA}$ cells were previously generated in our lab as stable cell lines for the cell surface expression of hFcRn and HLA, respectively [21]. Since CD47 is also expressed on 293 T cells that might well contribute to the binding of the fusion proteins, binding studies in the presence of access CD47-His (250 ug/nl, Novoprotein, C321) at pH6.0 were included. As shown in Fig. 2d–f, while the fusion proteins had limited binding to 293TEGFP-hFcRn at pH 7.4 at concentrations as high as 10 ug/ml (Fig. 2d), both SIRPα-F8 and SIRPα-Ig showed dose dependent binding to $293T^{EGFP-hFcRn}$ at pH6.0, which was apparently partly mediated via CD47 and partly via FcRn (Fig. 2e, Suppl. Figure 1). The EC50 for SIRPα-F8 was about 0.95 ug/ml, while that of SIRPα-Ig with the natural Fc fragment was about 1.11 ug/ml (Fig. 2e). The binding to $293T^{EGFP-HLA}$ cells were used as controls (Fig. 2f).

The antagonist effects of SIRPα-F8 to cancer cell 'do not eat me' signal

The effects of SIRPα-F8 antagonizing CD47 on cancer cells were evaluated by analyzing phagocytosis events using a high-content cellomics system using the co-culture system containing CD47 positive T lymphoblastoid leukemia CCRF-CEM cells and human monocytes derived-macrophages. CFSE labelled CCRF-CEM cells were cultured with PKH26 labelled macrophages in the presence of various proteins including SIRPα-F8. The phagocytic activities of macrophages engulfing cancer cells were imaged and quantified as shown in (Fig. 3a–h).

Both SIPRα-His (Fig. 3e) and SIRPα-F8 (Fig. 3f) were not capable of inducing phagocytosis by themselves. But SIRPα-Ig resulted in active phagocytosis shown as the heavily swollen macrophages containing engulfed tumor cells (Fig. 3d). For comparison, the commercial CD47 blocking antibody B6H12 triggered highly significant phagocytosis (Fig. 3c), but the non-blocking CD47 antibody 2D3 did not (Fig. 3b). These observations confirmed that monomeric SIPRα antagonists could only block the "do not eat me" signal but would not trigger significant effector functions. Similar observations were obtained in studies using Raji cells (Fig. 3i). Only SIRPα-Ig as a dimer triggered strong phagocytosis, while all the monomers including SIRPα-F8, F8, SIRPα-his and SIRPα-F0 were not effective by themselves.

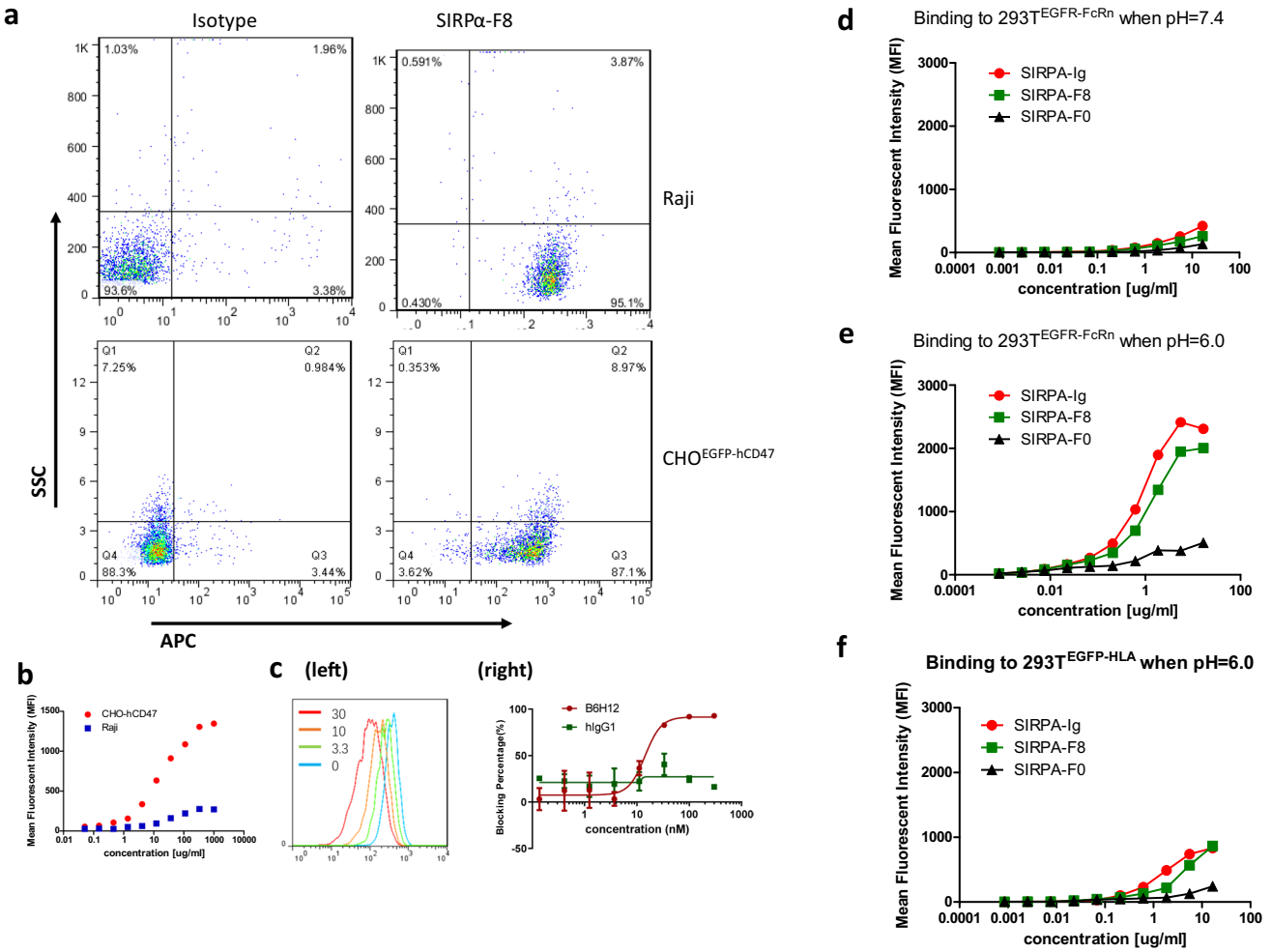

Fig. 2 Characterizations of the binding capabilities of SIRPα-F8 to CD47 and hFcRn expression cells. **a** FACS plots of SIRPα-F8 (111 nM concentration) binding to Raji cells and $CHO^{EGFP-hCD47}$ cells. **b** SIRPα-F8 binding to Raji cells and $CHO^{EGFP-hCD47}$ cells. The EC50 was 39.7 nM and 18.3 nM, respectively. **c** Characterization of SIRPα-F8 binding to Raji cells in the presence of 100 nM biotinylated SIRPα-Ig (left) or various concentrations of CD47 antibody B6H12 (right). The concentrations of SIRPα-F8 shown in the left figure were 0, 30, 10, 3.3 mg/ml. The concentrations of SIRPα-F8 in the right figure was fixed at 560 nM. **d** SIRPα-F8 and SIRPα-Ig binding to $293T^{EGFP-hFcRn}$ cells in the presence of SIRPa-His at pH 7.4. **e** SIRPα-F8 and SIRPα-Ig binding to $293T^{EGFP-hFcRn}$ cells in the presence of SIRPa-His at pH 6.0. **f** SIRPα-F8 and SIRPα-Ig binding to $293T^{EGFP-HLA}$ cells in the presence of SIRPa-His at pH = 6.0

However, SIRPα-F8 was able to significantly promote phagocytic activities of a therapeutic mAb recognizing tumor cell surface antigen. Anti-CD20 mAb is a tumor-opsonizing antibody that had moderate phagocytic activities when added alone (Figs. 3i, 4a). But with the addition of SIRPα-F8, the blockage of CD47-induced SIRPα signaling resulted in significantly higher ADCP activities of anti-CD20 as shown in (Fig. 4a).

The tumor inhibition effect of SIRPα-F8 in combination with anti-CD20 mAbs

The SIRPα-F8 activities in vivo were tested in a Raji cell xenograft model in NOD/SCID mice (Fig. 4b). The SIRPα-F8 was injected directly into tumor tissues because the F8 domain was only effective towards human FcRn. As shown in Fig. 4c, SIRPα-F8 alone did not affect tumor growth. But SIRPα-F8 combined with anti-CD20 mAbs resulted in significant inhibition of tumor growth comparing to the vehicle control group (Fig. 4c). The difference between the combination group and the anti-CD20 mAb only group was not as significant. We also calculated the TGI index of the different groups (Fig. 4d). The combination group was about 70% and the anti-CD20 mAbs group was only about 31%.

In vivo pharmacokinetics study of SIRPα fusion protein in hFcRn knock-in mice

In order to evaluate the effect of the F8 domain, we tested the pharmacokinetic (PK) behavior of SIRPα-F8 in hFcRn

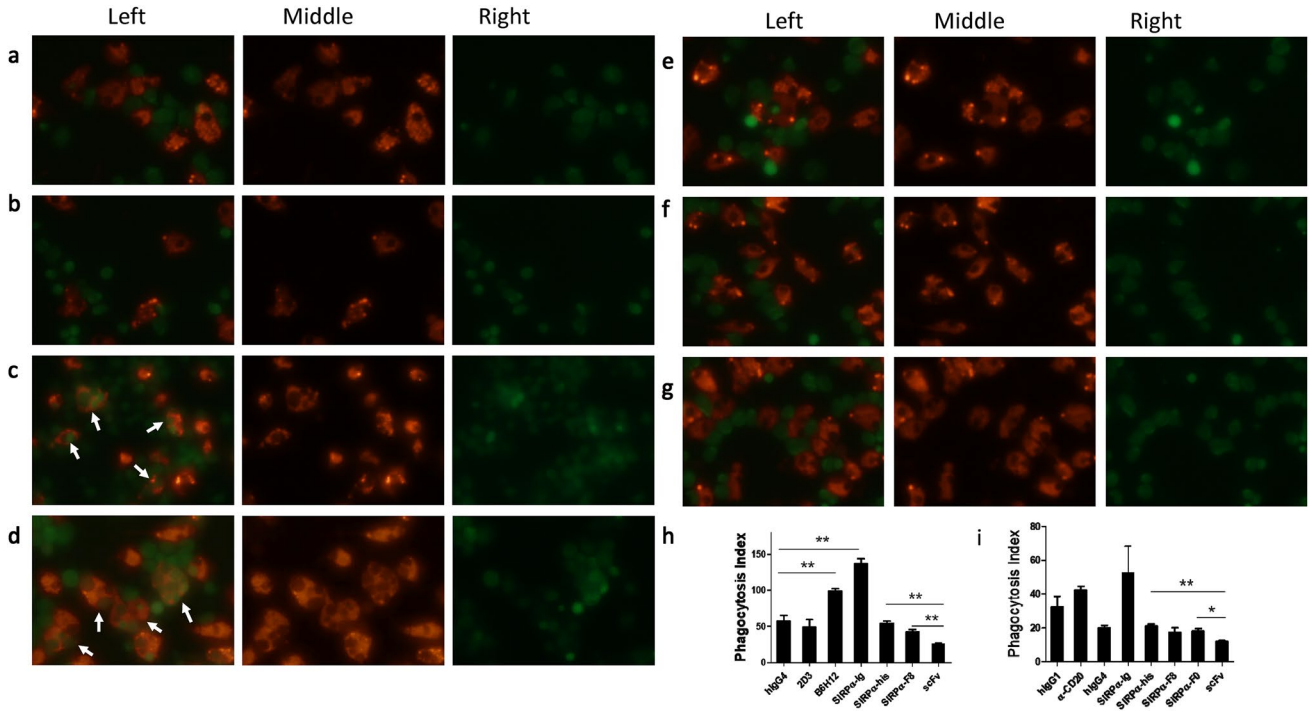

Fig. 3 CCRF- High-content Cellomics analysis of the phagocytic activities of human monocytes derived macrophages towards CCRF-TEM cells (**a**–**h**) and Raji cells (**i**). TEM cells were labeled with CFSE (green), and macrophages were labeled with PKH26 (red). There were co-cultured in the presence of various proteins at the same concentration of 10 mg/ml. Representative images were shown, and the arrows were added to mark macrophage engulfment of CCRF-CEM cells. **a** Isotype hIgG4, (**b**) the 2D3 antibody, (**c**) B6H12, (**d**) SIRPα-Ig, (**e**) SIRPα-his, (**f**) SIRPα-F8, (**g**) F8. **h** Summary of the phagocytosis index of CCRF-TEM cells in the presence of various protein antagonists. **i** Summary of the phagocytosis index of Raji cells in the presence of various protein antagonists. The experiment was repeated 3 times. $^{*}p < 0.05$, $^{**}p < 0.01$ were determined by *t* test

knock-in mice. SIRPα-F0 with the same molecular weight was used as the negative control. Proteins were administered in a single bolus injection. The plasma concentration following the injection was monitored for 21 days and plotted in (Fig. 5a). The calculated PK parameters were showed in (Fig. 5b). The MRT of SIRPα-F8 fusion protein was about 13.3 h in the hFcRn knock-in mouse. This is about 66 times longer than that of SIRPα-F0.

Discussion

In recent years, blockers of inhibitory immune checkpoints including PD-1 and CTLA-4 led most significant advances in anticancer therapies [22–24]. They also prompted the evaluation of other immune checkpoints that could be targeted. The "do not eat me" signal axis CD47-SIRPα has captured substantial attention [6, 12, 13]. Hu5F9-G4 was the first-in-human CD47 antibody tested in patients with relapsed or refractory solid tumors (NCT02216409) and AML (NCT02678338) [17], followed by CC-90002 (NCT02641002) [14] and SRF231 (NCT03512340) [16]. Alternatively, CD47 blocking decoy receptors based on SIRPα were also under development, including SIRPα-IgG1 Fc fusion (TTI-621) [25] and SIRPα-hIgG4 Fc fusion (ALX148) [18], There were also anti-SIRPα mAbs proposed for the potential treatment of various solid tumors [26, 27].

While all these CD47 antagonists were aimed to block the CD47-SIRPα axis signaling, there have been reports of toxicities considering the wide expression of CD47 in normal "self" cells. The most significant adverse effect using Hu5F9-G4 was reported to be anemia [17]. The CC-90002 clinical program was terminated also because of its narrow therapeutic window. TTI-622 switched to the use of IgG4 Fc which showed weaker ADCC and ADCP effects [15]. But the two binding sites on a single IgG format may still cause multivalent CD47 ligation on normal cells. The frequently reported side effects were leukopenia and thrombocytopenia. Weiskopf et al. suggested monovalent CD47 blockers would have lower avidity and could not trigger phagocytic activities by themselves [20]. Indeed in our phagocytosis assay in (Fig. 3), all the bivalent blockers including CD47 mAbs and SIRPα-Ig triggered significant phagocytosis by themselves, while all the monovalent binders including SIRPα-F8, SIRPα-his and SIRPα-F0 had no such effects

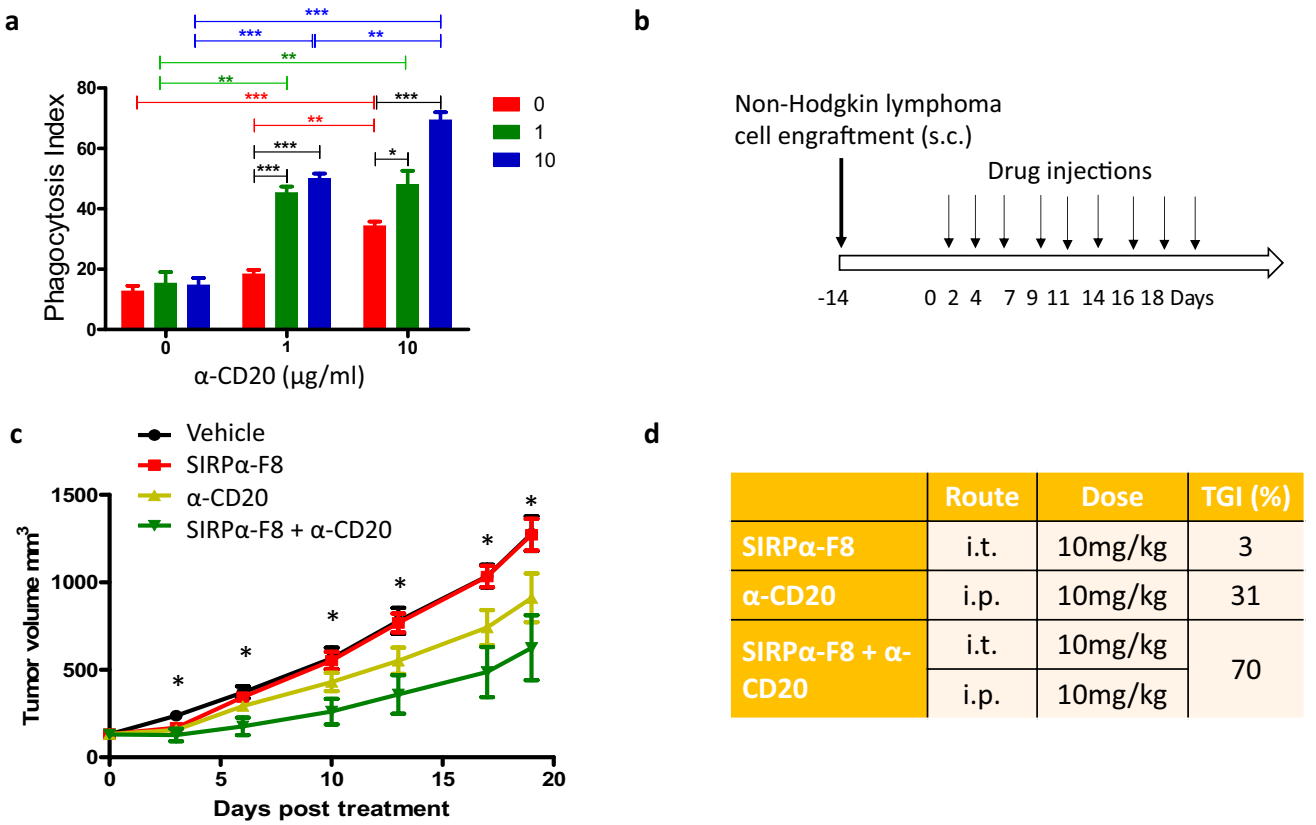

d

	Route	Dose	TGI (%)
SIRPα-F8	i.t.	10mg/kg	3
α-CD20	i.p.	10mg/kg	31
SIRPα-F8 + α-CD20	i.t.	10mg/kg	70
	i.p.	10mg/kg	

Fig. 4 The anti-tumor effects of SIRPα-F8 in combination with anti-CD20 mAb. **a** The phagocytosis indexes of human monocytes derived macrophages against Raji cells using both SIRPα-F8 and anti-CD20 antibody. The protein concentration was 0, 1 and 10 mg/ml respectively. The experiment was repeated 3 times. $*p<0.05$, $**p<0.01$, $***p<0.001$ were determined by *t* test. **b** The establishment of Raji cell derived xenograft model in NOD/SCID mouse and the treatment schedule. **c** Tumor growth curves of SIRPα-F8, anti-CD20 mAb, and the combination treatment groups. Error bar depicts standard deviation. $*p<0.05$ determined by t-test between vehicle and combination treatment groups. **d** Summary of the tumor growth inhibition (TGI) data at day 13 post treatment

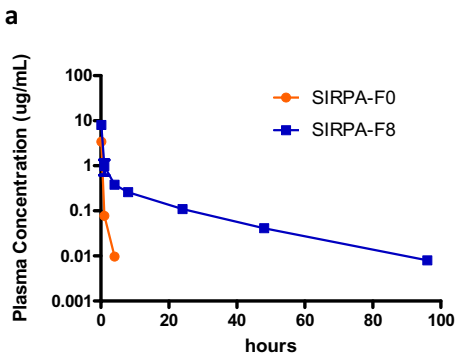

b

	β phase $T_{1/2}$ (hr)	AUC_{inf} (hr*ng/ml)	Cl (ml/hr/kg)	MRT (hr)
SIRPα-F0	0.53	2460.64	203.12	0.21
SIRPα-F8	11.14	14877.50	33.61	13.30

β phase $T_{1/2}$ (hr), elimination half-life; AUC, area under the plasma concentration curve; CL, total body clearance; MRT, mean residence time

Fig. 5 Characterizations of the pharmacokinetic behavior of SIRPα-F8 in hFcRn knock-in mice**. a** Measurements of SIRPα-F8 and SIRPα-F0 blood concentration over time. **b** PK parameters calculated: $T_{1/2}$ (hr): elimination half-life; *AUC* area under the plasma concentration curve; *CL* total body clearance; *MRT* mean residence time

(Fig. 3h–i). Therefore, we think they would be safer when exposed systemically in the presence of a deep antigen sink.

But the SIRPα domain by itself is too small and expected to have a very short residue life in vivo. Therefore, we proposed the fusion construct of SIRPα-F8 that included a 'recycle me' module in addition to the 'eat-me' module (Fig. 1d). F8 was previously developed in our lab with pH dependent binding affinities to human FcRn and we

showed that its circulation half-life in non-human primates was longer than 200 h [21]. Indeed as shown in (Fig. 5), SIRPα-F8 had a $T_{1/2}$ of 11.14 h in human FcRn knock-in mice, much longer than that of the FcRn unrelated control SIRPα-F0. But the Raji cell xenograft mice used in (Fig. 4) only expressed murine FcRn that's not homologous to human FcRn. We had to inject SIRPα-F8 intratumorally in the in vivo efficacy study in order to compensate for its short resident time in mice.

The anti-cancer activities of the SIRPα-F8 fusion protein was evaluated in combination with the anti-CD20 mAb. Most other CD47 blockers under development are also tested using similar combination regimen [6, 28]. The anti-tumor effects of Rituximab (anti-CD20 Mab) were mostly based on effector functions including FcR mediated opsonization and phagocytosis. In the presence of SIRPα-F8, significantly higher phagocytic activities were achieved by anti-CD20 in the tumor cell and macrophage co-culture model (Fig. 4a). The anti-tumor activities in vivo in the anti-CD20 and SIRPα-F8 combination group were also higher than the anti-CD20 mAb alone group (Fig. 4c, d). In the literature, Hu5F9-G4 was under testing for combinations with cetuximab (NCT02953782), azacytidine (NCT03248479), and rituximab (NCT02953509), similar for TTI-621, ALX148, and the anti-SIRPα antibody KWAR23. More advanced designs including bispecific antibodies targeting both CD47 and tumor cell antigens including CD19 and Mesothelin were also reported [29, 30]. Interestingly it is considered highly important to use the CD47 binding arm with lower affinity than the tumor antigen binding arm, in order to lower the possible side effects on red blood cells and platelets.

In addition to the "eat me" signaling effect, there may other mechanism involved in the anti-tumor activities of CD47 antagonists. One lab showed that the anti-tumor effects required dendritic cells in immune-competent mice, and they were abrogated in T cell deficient mice [31]. Another study suggested CD47 blockage could induce cell apoptosis directly [33]. CD47 blockade could also result in sustainable adaptive immune responses [32]. The importances of the CD47-SIRPα checkpoint pathway are still being explored. They are also under development for combinations with PD-1 checkpoint inhibitors including Nivolumab (NCT02663518) and Pembrolizumab (NCT03013218).

The SIRPα-F8 fusion protein we described weighted only 45 kD, one-third of that of an IgG, while the in vivo half-life and plasma concentrations would be higher. The small size would have advantages in distribution and diffusion in solid tumor tissues [36], while the improvements of half-life and systemic exposure improve the efficacy [34, 35]. Furthermore, the monovalent blocking mode helps to minimize the side effects toward normal self-cells. They will be used in combination with cancer cell targeted mAbs to ensure the specificity of the phagocytic activities. All combined, we hope the proposed strategy will have significantly widened therapeutic window and enable treatment of solid tumor tissues.

Acknowledgments We thank Hongtao Lu and Lei Shi for helpful discussions. We also thank Shou Li and Xu Fang for their help with the $CHO^{EGFP-hCD47}$ cell line and the phagocytosis assays. We appreciated Xinyan Lu for her help with statistical analysis and Yanbing Ma for his help with the protein structure simulation.

Author contributions Fenglan Wu designed the experiments, did the experiment and drafted the manuscript. Yangsheng Qiu participated in the experiment design and helped with the FcRn binding study. Yuhong Xu directed the experiment design and wrote the manuscript.

Funding This study was sponsored by the National Natural Science Foundation of China (NSFC) No. 81690262.

Compliance with ethical standards

Conflict of interest The authors declare no potential conflict of interest.

Ethical approval and ethical standards The animal study protocol A2016014 was approved by the Experimental Animal Management Committee and Experimental Animal Ethics Committee of Shanghai Jiao Tong University following the recommendations in the Guide for the Care and Use of Laboratory Animals (Eighth Edition) and relevant Chinese laws and regulations.

Animal source NOD/SCID mice were purchased from Beijing HFK Bioscience. FcRn humanized C57BL/6 mice were purchased from Beijing Biocytogen.

Cell line authentication HEK293-6E suspension cells expression system was purchased from ThermoFisher. CHO cells, Raji cells and CCRF-CEM cells were purchased from ATCC. PBMCs were purchased from all cells.

References

1. Pardoll DM (2012) The Blockade of immune checkpoints in cancer immunotherapy. Nat Rev Cancer 12:252–264. https://doi.org/10.1038/nrc3239
2. Weber JS, D'Angelo SP, Minor D et al (2015) Nivolumab versus chemotherapy in patients with advanced melanoma who progressed after anti-CTLA-4 treatment (CheckMate 037): a randomised, controlled, open-label, Phase 3 trial. Lancet Oncol 16:375–384. https://doi.org/10.1016/S1470-2045(15)70076-8
3. Ledford H (2011) Melanoma drug wins US approval. Nature 471(7340):561. https://doi.org/10.1038/471561a
4. Rizvi NA, Mazières J, Planchard D et al (2015) Activity and safety of Nivolumab, an anti-PD-1 immune checkpoint inhibitor, for patients with advanced, refractory squamous non-small-cell lung cancer (CheckMate 063): a phase 2, single-arm trial. Lancet Oncol 16:257–265. https://doi.org/10.1016/S1470-2045(15)70054-9
5. Weiskopf K, Weissman IL (2015) Macrophages are critical effectors of antibody therapies for cancer. Mabs 7:303–310. https://doi.org/10.1080/19420862.2015.1011450

6. Zhao XW, van Beek EM, Schornagel K et al (2011) CD47-signal regulatory protein-α (SIRPα) interactions form a barrier for antibody-mediated tumor cell destruction. PNAS 108:18343–18347. https://doi.org/10.1073/pnas.1106550108
7. Murata Y, Kotani T, Ohnishi H, Matozaki T (2014) The CD47-SIRP signalling system: it is physiological roles and therapeutic application. J Biochem 155:335–344. https://doi.org/10.1093/jb/mvu017
8. Matlung HL, Szilagyi K, Barclay NA, van den Berg TK (2017) The CD47-SIRPalpha signaling axis as an innate immune checkpoint in cancer. Immunol Rev 276:145–164. https://doi.org/10.1111/imr.12527
9. Barclay AN, Van den Berg TK (2014) The Interaction between signal regulatory protein alpha (SIRPalpha) and CD47: structure, function, and therapeutic target. Annu Rev Immunol 32:25–50. https://doi.org/10.1146/annurev-immunol-032713-120142
10. Campbell IG, Freemont PS, Foulkes W, Trowsdale J (1992) An ovarian tumor marker with homology to vaccinia virus contains an IgV-like region and multiple transmembrane domains. Cancer Res 52:5416–5420
11. Majeti R, Chao MP, Alizadeh AA, Pang WW, Jaiswal S, Gibbs KJ, van Rooijen N, Weissman IL (2009) CD47 is an adverse prognostic factor and therapeutic antibody target on human acute myeloid leukemia stem cells. Cell 138:286–299. https://doi.org/10.1016/j.cell.2009.05.045
12. Jaiswal S, Jamieson CH, Pang WW, Park CY, Chao MP, Majeti R, Traver D, van Rooijen N, Weissman IL (2009) CD47 is upregulated on circulating hematopoietic stem cells and leukemia cells to avoid phagocytosis. Cell 138:271–285. https://doi.org/10.1016/j.cell.2009.05.046
13. Serena G, Inti Z, Christian S, Aurel P, Adrian FO, Yara B (2015) CD47 protein expression in acute myeloid leukemia: a tissuemicroarray-based analysis. Leuk Res 39:749–756. https://doi.org/10.1016/j.leukres.2015.04.007
14. Rama KN, Hardik M, Lilly W et al (2017) Abstract 4694 The humanized anti-CD47 monclonal antibody, CC-90002, has antitumor activity in Vitro and in Vivo. Cancer Res 77:13. https://doi.org/10.1158/1538-7445.AM2017-4694
15. Liu J, Wang L, Zhao F, Tseng S et al (2015) Pre-clinical development of a humanized anti-CD47 antibody with anti-cancer therapeutic potential. PLoS ONE 10:e0137345. https://doi.org/10.1371/journal.pone.0137345
16. Pamela MH, Emmanuel N, Ammar A et al (2016) CD47 monoclonal antibody SRF231 is a potent inducer of macrophage-mediated tumor cell phagocytosis and reduces tumor burden in murine models of hematologic malignancies. Blood 128:1843. https://doi.org/10.1182/blood.V128.22.1843.1843
17. Advani R, Flinn I, Popplewell L et al (2018) CD47 blockade by Hu5F9-G4 and Rituximab in non-Hodgkin's lymphoma. N Engl J Med 379:1711–1721. https://doi.org/10.1056/NEJMoa1807315
18. Nehal JL, Patricia LR, Navid H et al (2018) A Phase 1 study of ALX148, a CD47 blocker, alone and in combination with established anticancer antibodies in patients with advanced malignancy and non-Hodgkin lymphoma. J Clin Oncol 36:30–68. https://doi.org/10.1200/JCO.2018.36.15_suppl.3068
19. Stephen A, Robert WC, Ian WF, Michael BM, Owen AC, Lisa DS, Meghan I, Penka SP, Robert AU, Eric LS (2016) A Phase 1 study of TTI-621 a novel immune checkpoint inhibitor targeting CD47 in patients with relapsed or refractory hematologic malignancies. Blood 128:1812. https://doi.org/10.1182/blood.V128.22.1812.1812
20. Weiskopf K, Ring AM, Ho CCM, Volkmer JP, Levin AM, Volkmer AK, Ozkan E, Fernhoff NB, van de Rijn M, Weissman IL, Garcia KC (2013) Engineered SIRP variants as immunotherapeutic adjuvants to anticancer antibodies. Science 341:88–91. https://doi.org/10.1126/science.1238856
21. Qiu Y, Lv W, Xu M, Xu Y (2016) Single chain antibody fragments with pH dependent binding to FcRn enabled prolonged circulation of therapeutic peptide in vivo. J Control Release 229:37–47. https://doi.org/10.1016/j.jconrel.2016.03.017
22. Koury J, Lucero M, Cato C et al (2018) Immunotherapies: exploiting the immune system for cancer treatment. J Immunol Res eCollection 95:13. https://doi.org/10.1155/2018/9585614
23. Veillette A, Chen J (2018) SIRPα–CD47 immune checkpoint blockade in anticancer therapy. Trends Immunol 39:173–184. https://doi.org/10.1016/j.it.2017.12.005
24. Matozaki T, Murata Y, Okazawa H, Ohnishi H (2009) Functions and molecular mechanisms of the CD47–SIRPα signalling pathway. Trends Cell Biol 19:72–80. https://doi.org/10.1016/j.tcb.2008.12.001
25. Petrova PS, Viller NN, Wong M et al (2017) TTI-621 (SIRPαFc): A CD47-blocking innate immune checkpoint inhibitor with broad antitumor activity and minimal erythrocyte binding. Clin Cancer Res 23:1068–1079. https://doi.org/10.1158/1078-0432.CCR-16-1700
26. Justine D, Vanessa G, Aurore M, Sabrina P, Bernard V, Nicolas P (2018) Abstract 1753 SIRPa inhibition monotherapy leads to dramatic change in solid tumor microenvironment and prevents metastasis development. Cancer Res 78:2. https://doi.org/10.1158/1538-7445.AM2018-1753
27. Ring NG, Herndler-Brandstetter D, Weiskopf K et al (2017) Anti-SIRPα Antibody immunotherapy enhances neutrophil and macrophage antitumor activity. PNAS 114:E10578–E10585. https://doi.org/10.1073/pnas.1710877114
28. Chao MP, Alizadeh AA, Tang C et al (2010) Anti-CD47 antibody synergizes with Rituximab to promote phagocytosis and eradicate non-Hodgkin lymphoma. Cell 142:699–713. https://doi.org/10.1016/j.cell.2010.07.044
29. Piccione EC, Juarez S, Liu J, Tseng S, Ryan CE, Narayanan C, Wang L, Weiskopf K, Majeti R (2015) A bispecific antibody targeting CD47 and CD20 selectively binds and eliminates dual antigen expressing lymphoma cells. Mabs 7:946–956. https://doi.org/10.1080/19420862.2015.1062192
30. Buatois V, Johnson Z, Salgado-Pires S et al (2018) Preclinical development of a bispecific antibody that safely and effectively targets CD19 and CD47 for the treatment of B-Cell lymphoma and leukemia. Mol Cancer Ther 17:1739–1751. https://doi.org/10.1158/1535-7163.MCT-17-1095
31. Liu X, Pu Y, Cron K, Deng L, Kline J, Frazier WA, Xu H, Peng H, Fu YX, Xu MM (2015) CD47 blockade triggers T cell-mediated destruction of immunogenic tumors. Nat Med 21:1209–1215. https://doi.org/10.1038/nm.3931
32. Sockolosky JT, Dougan M, Ingram JR, Ho CCM, Kauke MJ, Almo SC, Ploegh HL, Garcia KC (2016) Durable antitumor responses to CD47 blockade require adaptive immune stimulation. PNAS 113:E2646–E2654. https://doi.org/10.1073/pnas.1604268113
33. Pettersen RD, Hestdal K, Olafsen MK, Lie SO, Lindberg FP (1999) CD47 signals T Cell death. J Immunol 162:7031–7040. https://doi.org/10.1073/pnas.1604268113
34. Zalevsky J, Chamberlain AK, Horton HM et al (2010) Enhanced antibody half-life improves in vivo activity. Nat Biotechnol 28:157–159. https://doi.org/10.1038/nbt.1601
35. Hamblett KJ, Le T, Rock BM et al (2016) Altering antibody-drug conjugate binding to the neonatal Fc receptor impacts efficacy and tolerability. Mol Pharm 13:2387–2396. https://doi.org/10.1021/acs.molpharmaceut.6b00153
36. Stefan W, Anthony JT, Qin D, Seiichi O, Julie A, Warren CW (2016) Analysis of nanoparticle delivery to tumours. Nat Rev Mater 1:16014. https://doi.org/10.1038/natrevmats.2016.14